Synthesis and In Vivo Evaluation of p-^{18}F-Fluorohippurate as a New Radiopharmaceutical for Assessment of Renal Function by PET

Vibhudutta Awasthi, Gopal Pathuri, Hrushikesh B. Agashe, and Hariprasad Gali

Department of Pharmaceutical Sciences, The University of Oklahoma College of Pharmacy, Oklahoma City, Oklahoma

The molecular structure of p-^{18}F-fluorohippurate (^{18}F-PFH) is similar to that of p-aminohippurate, a gold standard for the measurement of effective renal plasma flow. The objective of this study was to investigate ^{18}F-PFH as a new PET renal agent. **Methods:** ^{18}F-PFH was synthesized by reacting *N*-succinimidyl-4-^{18}F-fluorobenzoate (^{18}F-SFB) with glycine at 90°C (pH 8) for 20 min. In vitro stability was determined by incubating ^{18}F-PFH in fresh human plasma at 37°C for 60 min. In vivo stability was determined by high-performance liquid chromatography analysis of urine collected from a normal rat at 40 min after injection of ^{18}F-PFH. The plasma protein binding and erythrocyte uptake were determined using plasma collected from a normal rat at 5 min after injection of ^{18}F-PFH. The plasma clearance of ^{18}F-PFH was determined using a single-injection clearance method in normal and probenecid-treated rats. Biodistribution studies were conducted in normal rats at 10 min and 1 h after injection of ^{18}F-PFH. Dynamic PET/CT studies were conducted in normal rats injected with ^{18}F-PFH. **Results:** In normal rats, the plasma clearance of ^{18}F-PFH was 4.11 ± 1.09 mL/min/100 g, which reduced by approximately 50% ($P = 0.03$) to 2.01 ± 0.08 mL/min/100 g in probenecid-treated rats. About 45.3% of ^{18}F-PFH was found to associate with plasma proteins in vivo in normal rats. Biodistribution studies of ^{18}F-PFH in normal rats showed 72.1 ± 6.4 percentage injected dose and 88.6 ± 6.2 percentage injected dose, respectively, in urine at 10 min and 1 h after injection. The uptake in other organs was negligible. High-performance liquid chromatography analysis of urine collected from a rat at 40 min after injection of ^{18}F-PFH indicated that it was excreted intact, with no metabolic products. Dynamic PET revealed a rapid clearance of ^{18}F-PFH through the renal–urinary pathway. The PET-derived renograms revealed a time to peak activity of 3.0 ± 1.0 min. **Conclusion:** These combined results warrant further investigation of ^{18}F-PFH as a radiopharmaceutical for the assessment of renal function by PET.

Key Words: PET; radiopharmaceuticals; renal; ERPF; renal function; renogram

Clinical PET is capable of providing excellent spatial resolution and absolute quantitative measurements; however, its use in the assessment of renal function has not been explored in the clinical setting. A few research studies have been conducted for the assessment of renal perfusion and glomerular filtration rate by PET. The corresponding radiotracers included ^{15}O-H$_2$O, ^{13}N-NH$_3$, ^{82}Rb-Rb$^+$, ^{62}Cu-Cu(II)pyruvaldehyde bis-(*N*-4-methylthiosemicarbazonato), and ^{62}Cu-Cu(II)ethylglyoxal bis(thiosemicarbazone) for renal perfusion studies [1–3] and ^{68}Ga-Ga-ethylenediaminetetraacetic acid, ^{55}Co-Co-ethylenediaminetetraacetic acid, and ^{18}F-F$^-$ for glomerular filtration rate studies [3–7]. In addition to drawbacks such as cost and availability, the clinical use of these radiotracers is limited by problems such as a short 2-min decay half-life (^{15}O-H$_2$O) or the high affinity of ^{18}F-F$^-$ toward bone, which is less than optimal in a renal imaging study. In this scenario, PET presents almost no competitive advantage over widely used planar γ-imaging for functional imaging of kidneys.

^{99m}Tc-diethylenetriamine pentaacetic acid (^{99m}Tc-DTPA)– and ^{99m}Tc-mercaptoacetyltriglycine (^{99m}Tc-MAG3)–based planar γ-imaging remain the nuclear imaging techniques of choice for the clinical evaluation of renal function and renography [8–13]. ^{99m}Tc-DTPA is exclusively cleared from plasma by glomerular filtration, a property that makes it useful at estimating the glomerular filtration rate [8,9]. However, its renal extraction efficiency is only 20% (the filtration fraction) [9], making the resultant images carry a low target-to-background ratio, especially in a dynamic acquisition of high frequency in patients with poor renal function. In comparison, ^{99m}Tc-MAG3 is almost exclusively cleared from plasma by tubular secretion, with a renal extraction efficiency approaching that of o-^{131}I-iodohippurate (^{131}I-OIH) [10,11]. The higher renal extraction of ^{99m}Tc-MAG3 is responsible for the improved image quality as compared with that obtained from ^{99m}Tc-DTPA. At the same time, the clearance and renogram curves of ^{99m}Tc-MAG3 are similar to those of ^{131}I-OIH, the gold standard, with less than ideal imaging characteristics.

In this article, we present our preclinical work toward the development of an ^{18}F-based renal imaging radiopharmaceutical, the biologic properties of which (compared with

[99mTc-MAG3] may be closer to [131I]-OIH. We observed that the major metabolite of 4-[18F]-fluorobenzoic acid is excreted rapidly and exclusively in urine as *p*-[18F]-fluorohippurate ([18F]-PFH) *(14)*. It is known that benzoic acid derivatives are converted in vivo into hippuric acid derivatives via the glycine-conjugation pathway in the liver *(15,16)*. This observation prompted us to investigate the potential use of [18F]-PFH as a PET renal agent. We report the synthesis and initial in vivo evaluation of [18F]-PFH in a rat model.

MATERIALS AND METHODS

General

All chemicals obtained commercially were used without further purification. Ethyl 4-(trimethylammonium triflate)benzoate and *N*-succinimidyl-4-fluorobenzoate (SFB) were synthesized as previously reported *(17,18)*. No-carrier-added [18F]-F$^-$ was obtained from Midwest Medical Isotopes, Inc. Electrospray mass spectral analysis was performed by the University of Oklahoma Health Sciences Center Molecular Biology-Proteomics Facility. ^{1}H-NMR spectral analysis was performed on a Varian Mercury VX-300 NMR Spectrometer at the University of Oklahoma NMR Facility. Sprague–Dawley (175–200 g) female rats were purchased from Charles River Laboratories International, Inc. Small-animal PET/CT was conducted in the University of Oklahoma Health Sciences Center College of Pharmacy Small Animal Imaging Facility using a Flex X-O/X-PET/CT scanner (Gamma Medica-Ideas). All animal studies were conducted in accordance with the protocols approved by the University of Oklahoma Health Sciences Center Institutional Animal Care and Use Committee.

Reversed-phase high-performance liquid chromatography (HPLC) analyses of [18F]-labeled and nonradioactive analogs were performed on a Beckman System Gold HPLC equipped with a Beckman Model 126 pump, 166 absorption detector, and a Bioscan Model B-FC-300 radioactivity detector. HPLC solvents consisted of water containing 0.1% trifluoroacetic acid (solvent A) and acetonitrile containing 0.1% trifluoroacetic acid (solvent B). A Sonoma C_{18} (ES Industries; 10 μm, 10 nm [100 Å], 4.6 × 250 mm) column was used with a flow rate of 1.5 mL/min. The HPLC gradient system began with an initial solvent composition of 80% solvent A and 20% solvent B for 2 min, followed by a linear gradient to 0% solvent A and 100% solvent B in 15 min, after which the column was reequilibrated. The absorption detector was set at 254 nm.

Synthesis of PFH

SFB (12.5 mg, 52.7 μmol) in dimethylformamide (0.5 mL) and glycine (2 mg, 26.7 μmol) in dimethylformamide (0.5 mL) were reacted in the presence of diisopropylethylamine (50 μL) for 18 h at room temperature. The resultant PFH was purified by HPLC (retention time, 8:23 min) and lyophilized to give pure PFH as a white powder in a yield of 76% (4 mg). ^{1}H-NMR (D_2O, 300 MHz) δ (ppm) 3.99 (s, 2H), 7.09 (m, 2H), 7.70 (m, 2H). Electrospray mass spectrometry calculated m/z for $C_9H_8FNO_3$: 197.2; found: 195.9 ([M − H]$^-$).

Radiosynthesis of [18F]-SFB

[18F]-SFB was synthesized in 1 pot manually by slight modifications to a previously reported procedure *(19)*. [18F]-F$^-$ (259–925 MBq) dissolved in water (1–2 mL) was added to a 5-mL V-shaped-bottom vial containing 250 μL of Kryptofix 222 (K222) (20 mg/mL

in acetonitrile) and 50 μL of K_2CO_3 (20 mg/mL in water). The solvents were evaporated under a stream of nitrogen at 90°C. Azeotropic drying was repeated twice with 1-mL portions of acetonitrile to generate the anhydrous [K/K222][18F] complex.

Ethyl 4-(trimethylammonium triflate)benzoate (5.0 mg) dissolved in anhydrous acetonitrile (1 mL) was added to the dried [K/K222][18F] complex, and the reaction mixture was heated at 90°C sealed for 10 min to produce ethyl 4-[18F]-fluorobenzoate. The ethyl ester was subsequently hydrolyzed to tetrapropylammonium 4-[18F]-fluorobenzoate by adding 1 M tetrapropylammonium hydroxide (50 μL) and heating the reaction mixture at 90°C sealed for 5 min. Finally, *N,N,N′,N′*-tetramethyl-*O*-(*N*-succinimidyl) uronium hexafluorophosphate (12 mg) dissolved in acetonitrile (1 mL) was added, and the reaction mixture was heated at 90°C sealed for 10 min. The reaction mixture was passed through an Oro-Sep SCX cartridge (600 mg; ChromTech), a Sep-Pak Light Accell Plus QMA cartridge (130 mg; Waters), and a Sep-Pak Light Alumina N cartridge (130 mg; Waters) connected in series to remove the cationic and anionic organic impurities and unreacted [18F]-F$^-$. The cartridges were eluted with an additional 2.5 mL of acetonitrile. The solvent was removed under a stream of nitrogen at 90°C, and [18F]-SFB was redissolved in ethanol (100 μL). The decay-corrected radiochemical yield was 68%–72%, starting from [18F]-F$^-$ in 8 preparations. The radiochemical purity of [18F]-SFB was more than 99%, as determined by HPLC.

Radiosynthesis of [18F]-PFH

A solution (100 μL) of 0.5 M glycine in 0.1 M Na_2HPO_4 (pH 8.0) was added to the [18F]-SFB solution and reacted at 90°C for 20 min. Normal saline (400 μL) was added to the reaction mixture. The [18F]-PFH was purified by HPLC, and solvents were evaporated by purging nitrogen at 90°C. The dried HPLC–purified [18F]-PFH was reconstituted in normal saline and passed through a 0.2-μm syringe filter. The decay-corrected radiochemical yield for the glycine conjugation was 91%–95%. The radiochemical purity of the final product was more than 99%, as determined by HPLC.

In Vitro Stability

A sample of [18F]-PFH (~3.7 MBq, 25 μL) dissolved in normal saline was added to 1 mL of freshly collected human plasma in a culture tube and incubated at 37°C. An aliquot of the serum sample (2 μL) was injected into an HPLC column at 1 h to analyze the stability of [18F]-PFH in human plasma. The experiment was performed using 3 separate samples.

In Vivo Stability

A female Sprague–Dawley rat was anesthetized with 2% vaporized isoflurane and injected with a dose of approximately 3.7 MBq of [18F]-PFH in 250 μL of normal saline via the tail vein. The rat was euthanized at 40 min after injection, the bladder containing the urine was carefully excised, and the urine was collected from the bladder. An aliquot of the urine sample (10 μL) was injected into an HPLC column to analyze the in vivo stability of [18F]-PFH in the rat.

In Vivo Plasma Protein Binding (PPB) and Erythrocyte Uptake

Two normal female Sprague–Dawley rats (~220 g) were anesthetized with 2% vaporized isoflurane and injected with a dose of approximately 8.5 MBq of [18F]-PFH in 400 μL of normal saline via the tail vein. A sample of approximately 2.5 mL of blood was collected in a heparinized blood collection tube from each rat at 5 min after injection. The blood samples were immediately cen-

trifuged for 5 min, and plasma samples were collected. The PPB was determined by an ultrafiltration membrane system (20,21). A sample of 1 mL of plasma was added to Millipore Centrifree ultrafiltration tubes (molecular weight cutoff, 30,000) prerinsed with 500 μL of phosphate-buffered saline containing a 5 mg/mL solution of PFH. The ultrafiltration tubes were centrifuged at 1,667g for 45 min, and the ultrafiltrate was collected. The radioactivities associated with the plasma samples (50 μL) and ultrafiltrate samples (50 μL) were recorded on a Cobra II automated γ-counter (Packard Instruments). The radioactivity counts were corrected for the background and decay during the counting. PPB was calculated as (1 − [ultrafiltrate counts/plasma counts]) × 100. Nonspecific membrane binding was evaluated by centrifuging ^{18}F-PFH in normal saline and showed no significant (<0.5%) membrane binding.

The blood samples were placed in capillary tubes and centrifuged to determine the hematocrit. The concentration of radioactivity (counts/g) in the whole blood and red blood cell samples was determined. Percentage erythrocyte uptake was calculated as (counts/g in red blood cells×hematocrit)/(counts/g in whole blood). No correction was made for plasma trapped in the red blood cell samples. The PPB and erythrocyte uptake were reported as a mean value obtained from 2 rats.

Plasma Clearance

The plasma clearance of ^{18}F-PFH was determined using a single-injection clearance method as described by Blaufox et al. (22). Four normal female Sprague–Dawley rats (230–280 g) were used for these studies. A femoral artery catheter was used for withdrawal of blood samples at various sampling points. The catheter consisted of a 47-mm tip made with light wall PTFE tube (28 gauge) attached to 20 cm of Tygon tubing (23 gauge). The rat was anesthetized with 2% isoflurane in oxygen. The inside of the left thigh was shaved and disinfected. A 1-cm incision was made at the juncture of the abdomen and thigh. The femoral artery was isolated by blunt dissection and then irrigated with a few drops of 1% lidocaine. A section of artery (5–8 mm) was elevated, and a vertical slit was made by a sterile sharp blade. A catheter was placed inside the artery and tied to and secured against the thigh muscle. The catheter was flushed with a 20 U/mL solution of heparin–saline.

First, a probenecid-treatment study was performed, followed by a control study after 5 d of the first study on the same rats. During the 5-d waiting period, the femoral artery catheter was maintained with a heparin block and capped with a 23-gauge plug. Every second day, the catheter was flushed with saline, and the heparin block was reestablished. For the probenecid-treatment study, each rat was injected with probenecid (70 mg/kg) in 390 μL of normal saline through the tail vein under isoflurane anesthesia at approximately 10 min before injection of ^{18}F-PFH (2.4–3.0 MBq) in 240–450 μL of normal saline. For the control study, each rat was injected only with a dose of ^{18}F-PFH (2.4–3.0 MBq) in 240–450 μL of normal saline through the tail vein under isoflurane anesthesia. Blood samples of approximately 200 μL were collected at 2, 5, 10, 20, 30, 40, 50, and 60 min after injection of ^{18}F-PFH. Blood samples were collected through the femoral artery catheter in heparinized tubes. Blood samples were centrifuged for 5 min, and 50 μL of plasma were separated. The radioactivity associated with each plasma sample was counted on the automated γ-counter.

All of the plasma samples were decay-corrected, background-subtracted, and plotted on a semilogarithmic graph as radioactivity (counts per minute/mL) against time (min) in Excel (Microsoft). The terminal portion (40, 50, and 60 min time points) of each curve was fitted with a single component, which was subtracted from the early portion (2, 5, and 10 min time points) of the curve to yield a more rapid early component. Clearance was calculated from the plasma curve by the method of Sapirstein et al. (23):

$$\text{Clearance}(C) = \frac{\text{Dose} \times \text{b1b2}}{\text{Ab2} + \text{Bb1}},$$

where A and b1 are the intercept and slope, respectively, of the terminal slow component, and B and b2 are the intercept and slope, respectively, of the early rapid component of the plasma disappearance curve. This equation is based on a 2-compartment model in which the dose is injected into compartment 1, diffuses into compartment 2, and is excreted from compartment 1.

Biodistribution

Eight normal female Sprague–Dawley rats (200–220 g) were initially anesthetized with 2% isoflurane in oxygen at 2 L/min and injected with a dose of approximately 1.3 MBq of ^{18}F-PFH in 200 μL of normal saline via the tail vein. Rats were kept under anesthesia during the study with 1% isoflurane in oxygen at 2 L/min. The rats were euthanized at 10 min (4 rats) and 1 h (4 rats) after injection. The bladder (containing the urine) and the tissue and organ samples were excised. The urine was collected from the bladder in a counting tube. If a rat urinated during or before euthanization, then the urine was carefully absorbed onto an absorbent gauze sponge and added to the corresponding urine tube. The tissues and organs were washed with normal saline, dried by blotting on tissue paper, and transferred to preweighed tubes. The tissue and organ sample tubes were weighed again to obtain the sample weight. The radioactivity associated with each sample tube was measured on the automated γ-counter. An undiluted standard dose (10 μL) was counted along with the samples. The radioactivity counts (counts per minute) were corrected for the background and radioactive decay. The percentage injected dose (%ID) and %ID/g of each tissue and organ were calculated. The %ID in blood was estimated assuming a whole-blood volume of 6.5% of the total body weight. The radioactivity in the stomach and intestines includes their content.

Small-Animal PET/CT

Five normal female Sprague–Dawley rats (200–220 g) were anesthetized initially using 2% isoflurane in oxygen at 2 L/min, in a polypropylene induction chamber. When fully anesthetized, the animal was placed on the scanner bed, with a nose cone used to maintain anesthesia at 1% isoflurane in oxygen at 2 L/min. Body temperature was maintained at 37°C using a water-circulated pad under the animal. A dose of approximately 2.6 MBq of ^{18}F-PFH in 250 μL of normal saline was injected into the tail vein. Dynamic small-animal PET data were acquired over a period of 60 min after injection, followed by the acquisition of CT data over a period of 1 min. The PET data were reconstructed using a 2-dimensional filtered backprojection algorithm. The PET scan time was divided into ten 30-s time frames for the first 5 min, followed by a 30-s time frame at each 5-min interval (total, 21 frames for a total scan time of 60 min). Regions of interest (ROIs) were drawn over the kidneys and a subrenal background guided by CT images. Radioactivity within the ROIs of each frame was calculated. Radioactivity in kidney ROIs for each frame was decay-corrected and background-corrected using the subrenal background ROI. The time–activity curve of both

kidneys (renogram) was plotted from the kidney ROI activities in each frame. Renogram analysis was performed for each rat. The time to peak activity and time to half-maximal activity were averaged for left and right kidneys for each rat. The right kidney fraction for each rat was calculated by dividing the counts in the right kidney ROI by the sum of counts in both right and left kidney ROIs at peak activity.

Statistical Analysis

All results are expressed as the mean $\pm$ SD. To determine the statistical significance of differences between the 2 groups, comparisons were made with the 2-tailed Student t test for paired data; a P value of less than 0.05 was considered to be statistically significant.

RESULTS

Chemistry

Nonradioactive PFH was synthesized to use as a reference standard for characterizing radioactive ^{18}F-PFH by HPLC. PFH was characterized by electrospray mass spectrometry and ^{1}H-NMR spectroscopy. Both PFH and ^{18}F-PFH were synthesized using the same glycine conjugation reaction but with different conditions. The ^{18}F-SFB prosthetic group was synthesized as shown in Figure 1, by slight modifications to the literature procedure (19). The HPLC retention times of ^{18}F-SFB (radioactive detection) and cold SFB (ultraviolet detection) were identical, indicating the product formation. ^{18}F-SFB was quantitatively converted to ^{18}F-PFH using a 0.5 M glycine solution. The HPLC retention times of ^{18}F-PFH (radioactive detection) and cold PFH (ultraviolet detection) were identical, indicating the product formation as shown in Figure 2.

In vitro stability studies of ^{18}F-PFH in human plasma at 37°C indicated that it is stable over the tested period of 1 h, and no degradation products were observed. For the in vivo stability study, we collected only a urine sample from a rat injected with ^{18}F-PFH because it is excreted exclusively via the renal route. Figure 2 shows a typical high-performance chromatogram of the ^{18}F-PFH injected dose and urine sample collected at 40 min after injection. No metabolites of ^{18}F-PFH were detected in the urine sample, indicating that ^{18}F-PFH is also stable in vivo.

Biology

The PPB of ^{18}F-PFH was 45.3%, and erythrocyte uptake of ^{18}F-PFH was 16.5%. The plasma clearance of ^{18}F-PFH was 4.17 $\pm$ 1.13 mL/min/100 g in normal (control) rats, which reduced by approximately 50% ($P = 0.034$) to 2.06 $\pm$ 0.05 mL/min/100 g in probenecid-treated rats.

The biodistribution of ^{18}F-PFH in normal rats at 10 min and 1 h after injection is shown in Table 1. The blood clearance was rapid, with only 3.54% $\pm$ 0.14% and 0.31% $\pm$ 0.18% of the injected dose remaining in the blood at 10 min and 1 h after injection, respectively (Table 1). The activity of ^{18}F-PFH excreted in urine at 10 min and 1 h after injection was 72.1 $\pm$ 6.4 %ID and 88.6 $\pm$ 6.2 %ID, respectively (Table 1). Less than 0.5 %ID of ^{18}F-PFH was found to be collectively associated with the blood, heart, lungs, liver, and spleen at 1 h after injection (Table 1).

Renograms

Results from the PET-derived renograms obtained after ^{18}F-PFH administration in normal rats are summarized in Table 2. A representative renogram is shown in Figure 3. Average time to peak kidney activity was 3.0 $\pm$ 1.0 min, and average time to half-maximal activity was 5.6 $\pm$ 2.4 min. The average fraction of radioactive counts in the right kidney at peak maximum was 0.51 $\pm$ 0.06.

DISCUSSION

Noninvasive diagnostic procedures using radionuclides have been important in nuclear medicine practice for close to 3 decades (24). In classic physiologic imaging of renal function, glomerular filtration and tubular secretion are separately addressed by ^{99m}Tc-DTPA and ^{99m}Tc-MAG3, respectively
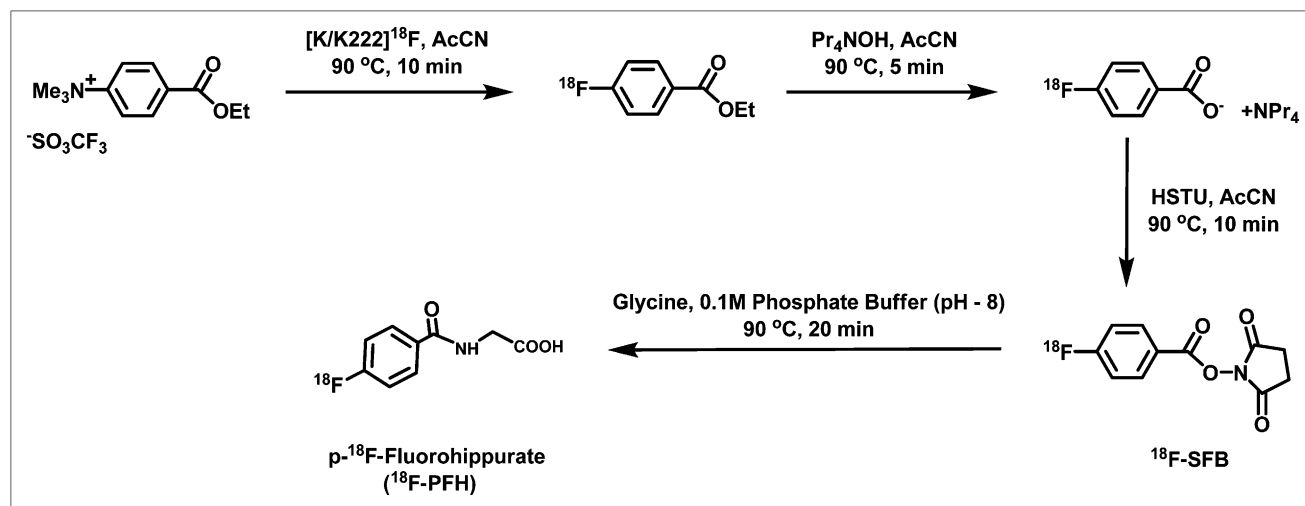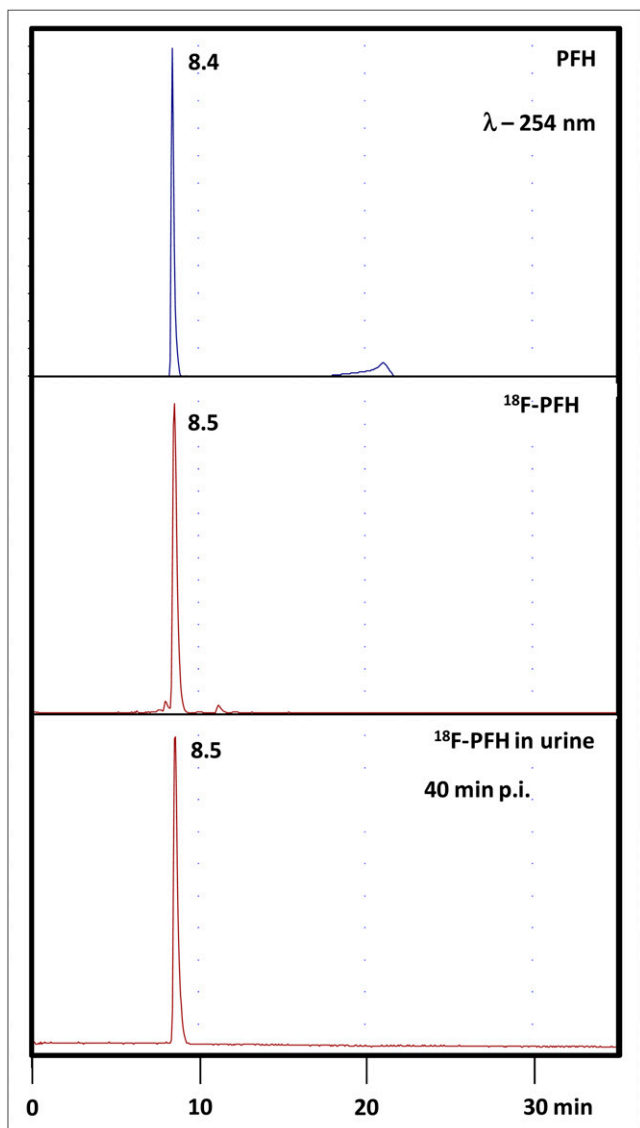

FIGURE 1. Radiosynthesis of ^{18}F-PFH.

FIGURE 2. High-performance chromatograms of cold PFH (A), ^{18}F-PFH (B), and rat urine (C) collected at 40 min after injection of ^{18}F-PFH. No metabolic products were observed in urine. p.i. = after injection.

(25). ^{99m}Tc-MAG3 has replaced the older ^{131}I-OIH that served as an imaging analog for the most original tubular compound *p*-aminohippurate (PAH) *(25,26)*. One of the goals in the radiopharmaceutics of renal agents has been to closely mimic the most original compound. For example, recently Taylor et al. have developed a new renal agent, ^{99m}Tc(CO)$_3$(NTA), which demonstrated pharmacokinetic properties and renogram parameters essentially identical to those of ^{131}I-OIH in healthy humans *(27)*. The structural and functional similarity of ^{131}I-OIH to PAH made ^{131}I-OIH the imaging gold standard for tubular function assessment. The relative advantages and disadvantages of these agents, and the reasons for the acceptability of ^{99m}Tc-MAG3 as a clinical tubular agent, are well reviewed *(11,13,28)*. While working on an unrelated project, we found that intravenously admin-

istered 4-^{18}F-fluorobenzoic acid was excreted rapidly and exclusively in urine as ^{18}F-PFH *(14)*. This observation, as well as the structural similarity of ^{18}F-PFH to PAH, prompted us to investigate ^{18}F-PFH as a potential PET renal agent. Therefore, we developed an efficient radiosynthesis method for preparing ^{18}F-PFH, as shown in Figure 1. ^{18}F-PFH demonstrated high stability with no metabolic degradation in both in vitro and in vivo conditions (Fig. 2). Thus, ^{18}F-PFH satisfies one of the important requirements for a renal agent—that is, no metabolic transformation in the body.

The PPB of ^{18}F-PFH was comparable to that of ^{131}I-OIH (45.3% vs. 44%, respectively), as reported in the literature *(21)*. However, the erythrocyte uptake of ^{18}F-PFH was lower than that of ^{131}I-OIH (16.5% vs. 35%, respectively), as reported in the literature *(21)*, which may be an advantage over ^{131}I-OIH because of lower background. The plasma clearance of ^{18}F-PFH was 4.11 ± 1.09 mL/min/100 g in normal rats, which is higher than the clearance of ^{125}I-OIH (2.11 mL/min/100 g) in normal rats observed by Blaufox et al. (determined using a single-injection clearance method *(22)*). However, the clearance of ^{18}F-PFH is comparable to that of ^{131}I-OIH (3.36 mL/min/100 g) and ^{99m}Tc-MAG3 (4.73 mL/min/100 g) in normal rats reported by Eshima et al., calculated from 3 clearance periods after reaching steady-state blood levels *(20)*. Other studies report ^{131}I-OIH plasma clearance of 2.17 mL/min/100 g *(29)* and 2.96 mL/min/100 g *(21)*; the plasma clearance of ^{99m}Tc-MAG3 has been reported as 2.84 mL/min/100 g in normal rats *(29)*. The source of variability in the reported values of ^{131}I-OIH and ^{99m}Tc-MAG3 plasma clearance is unknown. The plasma clearance of ^{18}F-PFH was reduced by approximately 50% in probenecid-treated rats. The reduced plasma clearance of ^{18}F-PFH in rats pretreated with probenecid demonstrates that renal excretion of this new agent may be principally by active tubular transport. Because the molecular structure of ^{18}F-PFH is similar to that of PAH, ^{18}F-PFH is likely transported by the same renal organic anion transporter 1 as PAH and ^{99m}Tc-MAG3 *(30)*. As in PAH, the carbonylglycine (-CO-NH-CH$_2$-COOH) side chain of ^{18}F-PFH may enable an efficacious fit with the receptor proteins of the tubular transport system *(31)*.

So that its plasma clearance would provide an accurate measurement of renal function, a renal agent must be exclusively excreted via the renal–urinary pathway to be used in humans. In this regard, ^{18}F-PFH displayed a rapid clearance from the blood exclusively through the renal–urinary pathway, with minimal retention (0.58 ± 0.30 %ID) in the kidneys at 1 h after injection (Table 1). The blood clearance and excretion of activity in urine of ^{18}F-PFH in normal rats are comparable to those of ^{131}I-OIH (0.27 ± 0.16 %ID vs. 0.5 ± 0.0 %ID, respectively, in blood and 88.6 ± 6.2 %ID vs. 91.4 ± 3.7 %ID, respectively, in urine at 1 h after injection) as reported by Lipowska et al. *(21)*. It is also important that the renal agent should not be cleared via the hepatobiliary pathway, to eliminate the high background activity in patients with impaired renal function. In this regard, the collective

TABLE 1
Biodistribution of ^{18}F-PFH in Rats at 10 Minutes and 1 Hour After Injection

Organ	10 min %ID	10 min %ID/g	1 h %ID	1 h %ID/g
Blood	3.54 ± 0.14	0.26 ± 0.01	0.31 ± 0.18	0.02 ± 0.01
Heart	0.06 ± 0.01	0.08 ± 0.01	0.01 ± 0.01	0.02 ± 0.02
Lung	0.21 ± 0.06	0.17 ± 0.04	0.02 ± 0.01	0.02 ± 0.01
Liver	0.57 ± 0.13	0.09 ± 0.01	0.09 ± 0.05	0.01 ± 0.01
Spleen	0.03 ± 0.01	0.06 ± 0.01	0.01 ± 0.00	0.01 ± 0.01
Kidney	3.98 ± 2.27	2.93 ± 1.52	0.58 ± 0.30	0.42 ± 0.23
Stomach	0.31 ± 0.23	0.12 ± 0.07	0.24 ± 0.18	0.06 ± 0.06
Intestine	0.95 ± 0.52	0.09 ± 0.03	0.60 ± 0.29	0.06 ± 0.03
Urine	72.1 ± 6.4	—	88.6 ± 6.2	—

Data are mean ± SD ($n = 4$).

activity of ^{18}F-PFH in the intestine and liver was less than 0.7 %ID at 1 h after injection (Table 1), suggesting that the hepatobiliary clearance of ^{18}F-PFH is minimal.

The small-animal dynamic PET performed on normal rats with ^{18}F-PFH indicated that the radiotracer was rapidly taken up by the kidney and cleared into bladder. Dynamic PET data were used to generate renograms (Fig. 3). The renogram data (Table 2) obtained here for ^{18}F-PFH are similar to those available in the literature for ^{131}I-OIH, further validating the functional similarity of ^{18}F-PFH to ^{131}I-OIH (32). One of the ideal characteristics of any ^{131}I-OIH replacement would be that the radiotracer is not fixed to the renal tissue, as can be evaluated by comparing the peaks of the time–activity curves (renograms) and the analyses of transit times (33). The time to peak kidney concentration for ^{18}F-PFH in normal rats was about 3 min (Table 2). This value is comparable to that reported for ^{131}I-OIH in a normal rat (34). After reaching the peak kidney concentration, the time to excrete 90% of the accumulated ^{18}F-PFH was about 12.5 min after injection. The PET/CT images presented in Figure 4 show the high uptake of radioactivity by the kidneys and its clearance into the urine or bladder within 30 min after injection, also confirming the exclusive renal excretion of ^{18}F-PFH. At 60 min after injection, the radioactivity was completely cleared from all other organs except the bladder.

## CONCLUSION

An efficient radiosynthesis method was developed for preparing ^{18}F-PFH using a classic ^{18}F-SFB prosthetic group. ^{18}F-PFH demonstrated high stability, with no metabolic degradation in either in vitro or in vivo conditions. The PPB of ^{18}F-PFH was found to be comparable to that of ^{131}I-OIH as reported in the literature, with relatively lower erythrocytic uptake. Initial biodistribution and dynamic PET studies in normal rats revealed a rapid clearance of ^{18}F-PFH exclusively through the renal–urinary pathway. The plasma clearance of ^{18}F-PFH was reduced by approximately 50% in probenecid-treated rats, suggesting that renal excretion may be principally by renal tubular secretion. These combined results warrant further investigation of ^{18}F-PFH as a radiopharmaceutical for the assessment of renal function by PET.

TABLE 2
### Renogram-Derived Data from Normal Rats Injected with ^{18}F-PFH

Time to peak activity (min)	Fraction right kidney	Time to half-maximal activity (min)
4.6	0.55	8.6
2.7	0.45	4.0
2.5	0.51	3.9
2.0	0.58	3.5
3.3	0.45	7.8
3.0 ± 1.0	0.51 ± 0.06	5.6 ± 2.4

Time data are averages of left and right kidneys of individual rats. Group data are presented as mean ± SD in final row. Time to half-maximal activity was calculated from injection time.
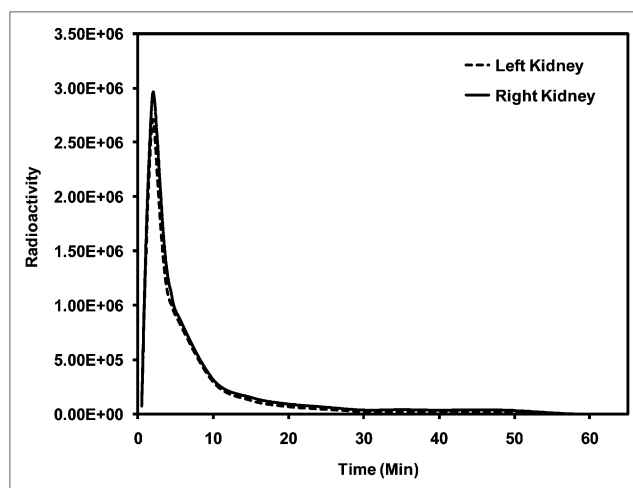
FIGURE 3. Kidney time–activity curves (renogram) from normal rat injected with ^{18}F-PFH (~2.6 MBq).
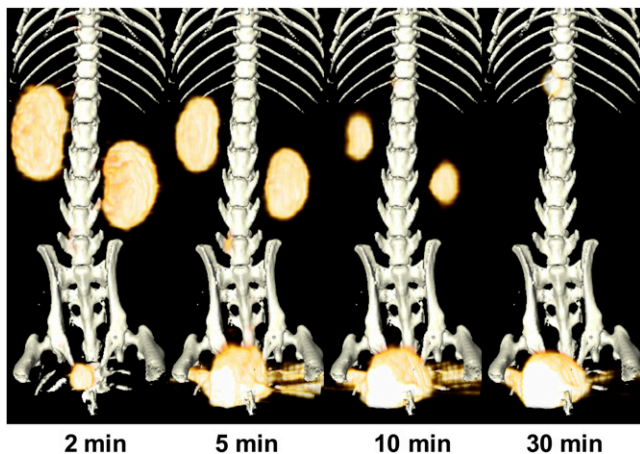
FIGURE 4. Lower abdominal maximum-intensity-projection PET/CT images of normal rat injected with ^{18}F-PFH (∼2.6 MBq). Within a few seconds of injection, radioactivity accumulated in kidneys, followed by start of its accrual in bladder within 2 min. By 30 min, almost all injected dose was excreted into bladder.

REFERENCES

1. Killion D, Nitzsche E, Choi Y, Schelbert H, Rosenthal JT. Positron emission tomography: a new method for determination of renal function. *J Urol.* 1993;150:1064–1068.
2. Shelton M, Green M, Mathias C, Welch M, Bergmann S. Assessment of regional myocardial and renal blood flow with copper-PTSM and positron emission tomography. *Circulation.* 1990;82:990–997.
3. Green MA, Mathias CJ, Willis LR, et al. Assessment of Cu-ETS as a PET radiopharmaceutical for evaluation of regional renal perfusion. *Nucl Med Biol.* 2007;34:247–255.
4. Yamashita M, Inaba T, Kawase Y, et al. Quantitative measurement of renal function using Ga-68-EDTA. *Tohoku J Exp Med.* 1988;155:207–208.
5. Goethals P, Volkaert A, Vandewielle C, Dierckx R, Lameire N. ^{55}Co-EDTA for renal imaging using positron emission tomography (PET): a feasibility study. *Nucl Med Biol.* 2000;27:77–81.
6. Schnöckel U, Reuter S, Stegger L, et al. Dynamic ^{18}F-fluoride small animal PET to noninvasively assess renal function in rats. *Eur J Nucl Med Mol Imaging.* 2008;35:2267–2274.
7. Szabo Z, Xia J, Mathews WB, Brown PR. Future direction of renal positron emission tomography. *Semin Nucl Med.* 2006;36:36–50.
8. Gates G. Glomerular filtration rate: estimation from fractional renal accumulation of ^{99m}Tc-DTPA (stannous). *AJR.* 1982;138:565–570.
9. Barbour GL, Crumb CK, Boyd CM, Reeves RD, Rastogi SP, Patterson RM. Comparison of inulin, iothalamate, and ^{99m}Tc-DTPA for measurement of glomerular filtration rate. *J Nucl Med.* 1976;17:317–320.
10. Esteves FP, Taylor A, Manatunga A, Folks RD, Krishnan M, Garcia EV. ^{99m}Tc-MAG3 renography: normal values for mag3 clearance and curve parameters, excretory parameters, and residual urine volume. *AJR.* 2006;187:W610–W617.
11. Itoh K. ^{99m}Tc-MAG3: review of pharmacokinetics, clinical application to renal diseases and quantification of renal function. *Ann Nucl Med.* 2001;15:179–190.
12. Taylor A Jr, Eshima D, Fritzberg AR, Christian PE, Kasina S. Comparison of iodine-131 OIH and technetium-99m MAG3 renal imaging in volunteers. *J Nucl Med.* 1986;27:795–803.
13. Jamar F, Barone R. Renal imaging. In: Baert A, Sartor K, Schiepers C, eds. *Diagnostic Nuclear Medicine.* Heidelberg, Germany: Springer; 2006:83–100.
14. Pathuri G, Agashe HB, Awasthi V, Gali H. Radiosynthesis and in vivo evaluation of a F-18-labeled pancreatic islet amyloid inhibitor. *J Labelled Comp Radiopharm.* 2010;53:186–191.
15. Hutt AJ, Caldwell J. Amino acid conjugation. In: Mulder GJ, ed. *Conjugation Reactions in Drug Metabolism.* London, U.K.: Taylor and Francis Ltd.; 1990:273–305.
16. Tremblay GC, Qureshi IA. The biochemistry and toxicology of benzoic acid metabolism and its relationship to the elimination of waste nitrogen. *Pharmacol Ther.* 1993;60:63–90.
17. Guhlke S, Coenen HH, Stöcklin G. Fluoroacylation agents based on small n.c.a. [^{18}F]fluorocarboxylic acids. *Appl Radiat Isot.* 1994;45:715–727.
18. Vaidyanathan G, Zalutsky MR. Synthesis of *N*-succinimidyl 4-[^{18}F]fluorobenzoate, an agent for labeling proteins and peptides with ^{18}F. *Nat Protoc.* 2006;1:1655–1661.
19. Tang G, Zeng W, Yu M, Kabalka G. Facile synthesis of *N*-succinimidyl 4-[^{18}F]fluorobenzoate ([^{18}F]SFB) for protein labeling. *J Labelled Comp Radiopharm.* 2008;51:68–71.
20. Eshima D, Taylor A Jr, Fritzberg AR, Kasina S, Hansen L, Sorenson JF. Animal evaluation of technetium-99m triamide mercaptide complexes as potential renal imaging agents. *J Nucl Med.* 1987;28:1180–1186.
21. Lipowska M, Marzilli LG, Taylor AT. ^{99m}Tc(CO)3-nitrilotriacetic acid: a new renal radiopharmaceutical showing pharmacokinetic properties in rats comparable to those of ^{131}I-OIH. *J Nucl Med.* 2009;50:454–460.
22. Blaufox MD, Guttmann RD, Merrill JP. Measurement of renal function in the rat with single injection clearances. *Am J Physiol.* 1967;212:629–632.
23. Sapirstein LA, Vidt DG, Mandel MJ, Hanusek G. Volumes of distribution and clearances of intravenously injected creatinine in the dog. *Am J Physiol.* 1955;181:330–336.
24. HE W, Fischman AJ. Nuclear imaging in the genitourinary tract: recent advances and future directions. *Radiol Clin North Am.* 2008;46:25–43.
25. Russell CD, Dubovsky EV. Measurement of renal function with radionuclides. *J Nucl Med.* 1989;30:2053–2057.
26. Blaufox MD. Procedures of choice in renal nuclear medicine. *J Nucl Med.* 1991;32:1301–1309.
27. Taylor AT, Lipowska M, Marzilli LG. ^{99m}Tc(CO)$_3$(NTA): a ^{99m}Tc renal tracer with pharmacokinetic properties comparable to those of ^{131}I-OIH in healthy volunteers. *J Nucl Med.* 2010;51:391–396.
28. Taylor AT, Lipowska M, Hansen L, Malveaux E, Marzilli LG. ^{99m}Tc-MAEC complexes: new renal radiopharmaceuticals combining characteristics of ^{99m}Tc-MAG3 and ^{99m}Tc-EC. *J Nucl Med.* 2004;45:885–891.
29. Fritzberg AR, Kasina S, Eshima D, Johnson DL. Synthesis and biological evaluation of technetium-99m MAG3 as a Hippuran replacement. *J Nucl Med.* 1986;27:111–116.
30. Shikano N, Kanai Y, Kawai K, Ishikawa N, Endou H. Transport of ^{99m}Tc-MAG3 via rat renal organic anion transporter 1. *J Nucl Med.* 2004;45:80–85.
31. Despopoulos A. A definition of substrate specificity in renal transport of organic anions. *J Theor Biol.* 1965;8:163–192.
32. Coveney JR, Robbins MS. Comparison of technetium-99m MAG3 kit with HPLC-purified technetium-99m MAG3 and OIH in Rats. *J Nucl Med.* 1987;28:1881–1887.
33. Jafri RA, Britton KE, Nimmon CC, et al. Technetium-99m MAG3, a comparison with iodine-123 and iodine-131 orthoiodohippurate, in patients with renal disorders. *J Nucl Med.* 1988;29:147–158.
34. Chauser BM, Hudson FR, Law MP. Renal function in the rat following irradiation. *Radiat Res.* 1976;67:86–97.